# A Pedagogical Illustration of the Determination of the Nature and Strength of Bonds in Crystalline Compounds from X-ray Diffraction and Infrared Spectroscopy Studies

**Pierre Couchot,[†] Sandrine Monney,[*,†] George D. Sturgeon,[‡] and Michael Knorr[†]**

*Département de Chimie, Université de Franche Comté, 25030 Besançon Cedex, France, sandrine.monney@univ-fcomte.fr, Department of Chemistry University of Nebraska, Lincoln, Nebraska 68588*

*Received June 29, 2000. Accepted October 17, 2000*

**Abstract:** This article describes a method used to teach students how X-ray crystallography and infrared spectroscopy analysis can be used to obtain information about the nature and strength of the bonding in the crystalline compounds $M^IM^{III}(SO_4)_2$ (with $M^I = K^+$, $Rb^+$, $Cs^+$ and $M^{III} = Al^{3+}$, $Cr^{3+}$, $Fe^{3+}$). These sulfates form an isomorphic series. The influences of specific $M^I$ and $M^{III}$ ions on the variation of the *a* and *c* parameters and on the position of IR absorption bands are described. Additionally, X-ray crystallography and infrared spectroscopy studies of the double sulfates $M^IM^{III}(SO_4)_2$ show students the existence of $[SO_4–M^{III}–SO_4]^-$ layers in the crystallized products; the covalent character of $M^{III}$–O attractions, which give cohesion in these layers; the existence of $M^I$ layers between $[SO_4–M^{III}–SO_4]^-$ layers, and the electrovalent character of $M^I$–O interactions.

## Introduction

The aim of this study is to teach students how X-ray crystallography and infrared spectroscopy analysis are used to get information about the nature and the strength of bonds in crystallized inorganic compounds. Indeed, these two techniques are often used to carry out parallel studies, in particular to study the metal to oxygen bond. [1–6]. In this article, the compounds under examination are the double sulfates: $M^IM^{III}(SO_4)_2$ ( with $M^I = K^+$, $Rb^+$, $Cs^+$ and $M^{III} = Al^{3+}$, $Cr^{3+}$, $Fe^{3+}$). They form an isomorphic series with a well-known structure. In comparison to the covalent S–O bonds, the $M^I$–O and the $M^{III}$–O bonds are sharply distinct. This fact allows a relatively straightforward discussion about X-ray crystallography and infrared spectroscopy analysis.

## Experimental

The aim of this work is not to repeat the depicted experiments, but rather to interpret the spectra analysis with the students. A brief description of the experimental conditions is provided for interested readers.

**Material and Sampling.** The $M^IM^{III}(SO_4)_2$ double sulfates are synthesized by mixing in equimolar quantities very finely pulverized anhydrous powders of $M^{III}_2(SO_4)_3$ and $M^I_2SO_4$ (with $M^{III} = Al^{3+}$, $Cr^{3+}$, $Fe^{3+}$, and $M^I = K^+$, $Rb^+$, $Cs^+$). The mixtures are pressed into pellets under a pressure of about 10 ton $cm^{-2}$. The pellets are placed in Pyrex-glass tubes. After evacuation, the tubes are sealed and then heated in an oven for 24 hours at 540 °C. Alternatively, these double sulfates could be obtained by dehydration, at 250°C, of the corresponding alums: $M^IM^{III}(SO_4)_2•12H_2O$; however, the products obtained by direct combination exhibit a better degree of crystallinity than the ones obtained via dehydration.

**Materials Characterization.** The powder X-ray diffractograms of the pure double sulfates have been recorded using a CPS INEL 120 instrument equipped with a multichannel detector. This apparatus covers the angular range of 20 to 120° and uses the $K_\alpha$ wavelength of copper ($\lambda$ = 1.54036 Å). Figure 1 shows the representative X-ray powder diffractogram of $RbFe(SO_4)$. The sharpness of the diffracted lines and the minimal background of the diffractograms prove the high crystallinity of the products.

The infrared spectra are recorded at 1300 to 200 $cm^{-1}$ on a Perkin–Elmer 225 infrared spectrometer (the samples are placed in Nujol suspension between KBr windows) and at 350 to 20 $cm^{-1}$ on an FTIR Polytec FIR-30 spectrometer (the samples are mixed with polyethylene to form pellets). Figures 2a and 2b show the representative infrared spectrum of $CsAl(SO_4)_2$

## Results, Interpretation, and Discussion

**Analysis of the X-ray Diffractograms.** $M^IM^{III}(SO_4)_2$ crystallizes in the hexagonal system, space group $P_{321}$ $\left(D_3^2\right)$ [7–10]. The structure of these salts is represented in Figures 3a and 3b. Figure 3a shows a single unit cell; Figure 3b shows assemblies of unit cells, stacked along the *a* and *c* directions. The *a* and *c* parameter values of some of these double sulfates are summarized in Table 1.

Table 2 gives the reduced coordinates of the ions $K^+$ and $Al^{3+}$; sulfur; special oxygens, $O^{IV}$; and general oxygens, $O^I$; as well as the symmetry and the multiplicity of the sites of these atoms or ions in $KAl(SO_4)_2$ [7].

The $M^I$ and $M^{III}$ ions form separate hexagonal layers. Sulfate ions are oriented alternately above and below the $M^{III}$ hexagonal layers with the $O^I$ general oxygens very close to the $M^{III}$ ions (the distance between $Al^{3+}$ and $O^I$ is 2.16 Å in

* Address correspondence to this author.
† Université de Franche Comté
‡ University of Nebraska

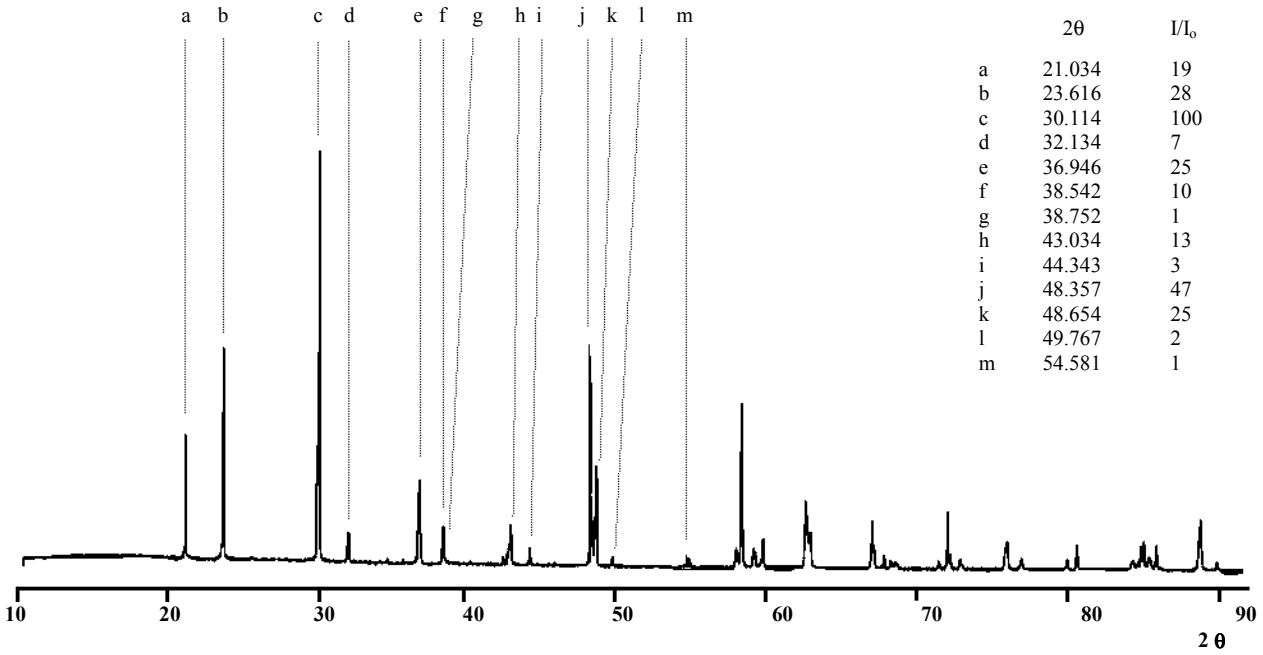


**Figure 1.** X-ray powder diffraction recording of Rb Fe $(SO_4)_2$.

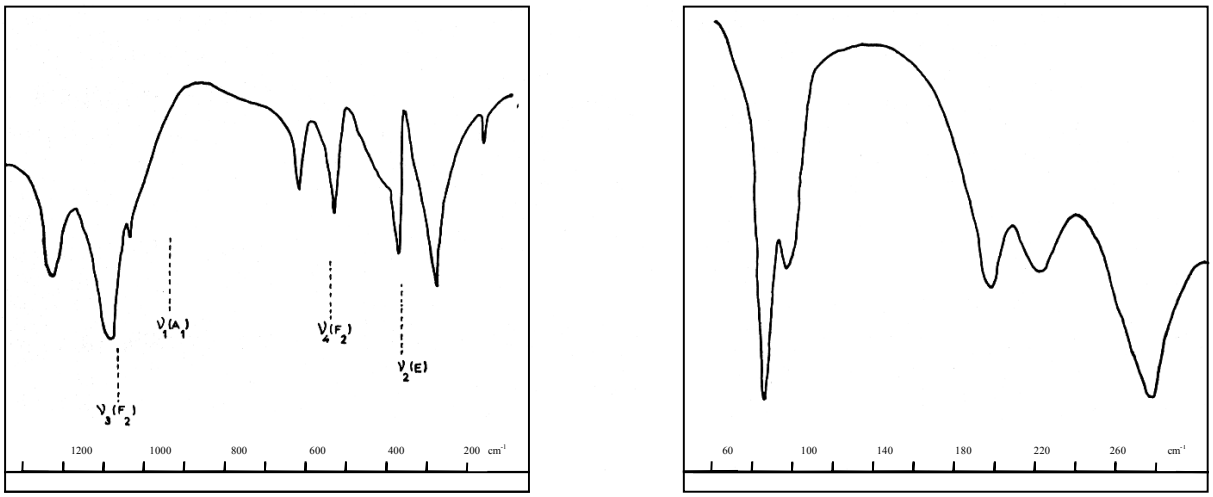


(a) Near IR (b) Far IR

**Figure 2.** Near and far infared spectra of $CsAl(SO_4)_2$.

$KAl(SO_4)_2$). In this way, the $M^{III}$ and $SO_4^{2-}$ ions form $[SO_4–M^{III}–SO_4]^-$layers.

The $O^{IV}$ special oxygens are near, and practically in the plane of, the $M^I$ ions. The $M^I$ monovalent cations are centered in very flattened trigonal antiprisms of which the six vertices are occupied by the special oxygens (distance $K^+–O^{IV}$ = 2.72 Å in $KAl(SO_4)_2$). In this way, the monovalent cations are surrounded by six $O^{IV}$ oxygens, almost in the same plane (Figure 3c). The trivalent $M^{III}$ cations are located within slightly distorted prisms with equilateral triangular bases; the vertices are occupied by the $O^I$ general oxygens (Figure 3d). In the case of a given $M^{III}$ cation, the *a* parameter changes slightly depending on the identity of the monovalent ion (Table 1).

The value of the *a* parameter represents the distance between the $M^{III}$ ions in the $[SO_4–M^{III}–SO_4]^-$ layers. In the case of a given $M^{III}$ cation, the dimensions of the $[SO_4–M^{III}–SO_4]^-$ layers are independent of the nature of the $M^I$ monovalent ions.

In contrast, the *c* parameter varies substantially as a function of the monovalent ion. The change in the *c* parameter confirms that the monovalent ions are positioned between the $[SO_4–M^{III}\text{-}SO_4]^-$ layers. This parameter grows with the $M^I$ monovalent ion's radius, *r* [11, 12]. The *c* parameter's variation, $\Delta c$, is very close to the variation in ionic radius $\Delta r$; yet, $\Delta c$ is always slightly greater than $2\Delta r$ (Table 1).

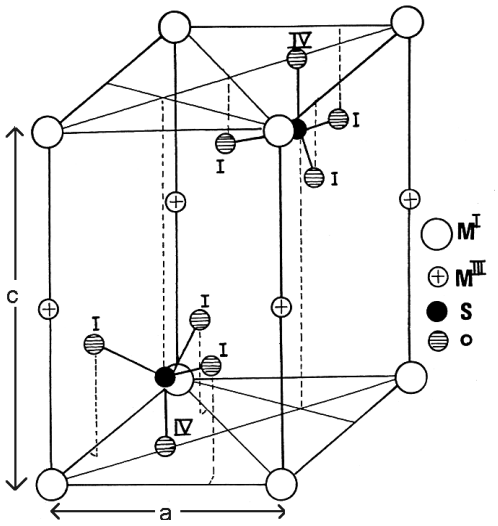


(a)

**Figure 3.** (a) Hexagonal cell of $M^IM^{III}(SO_4)_2$.

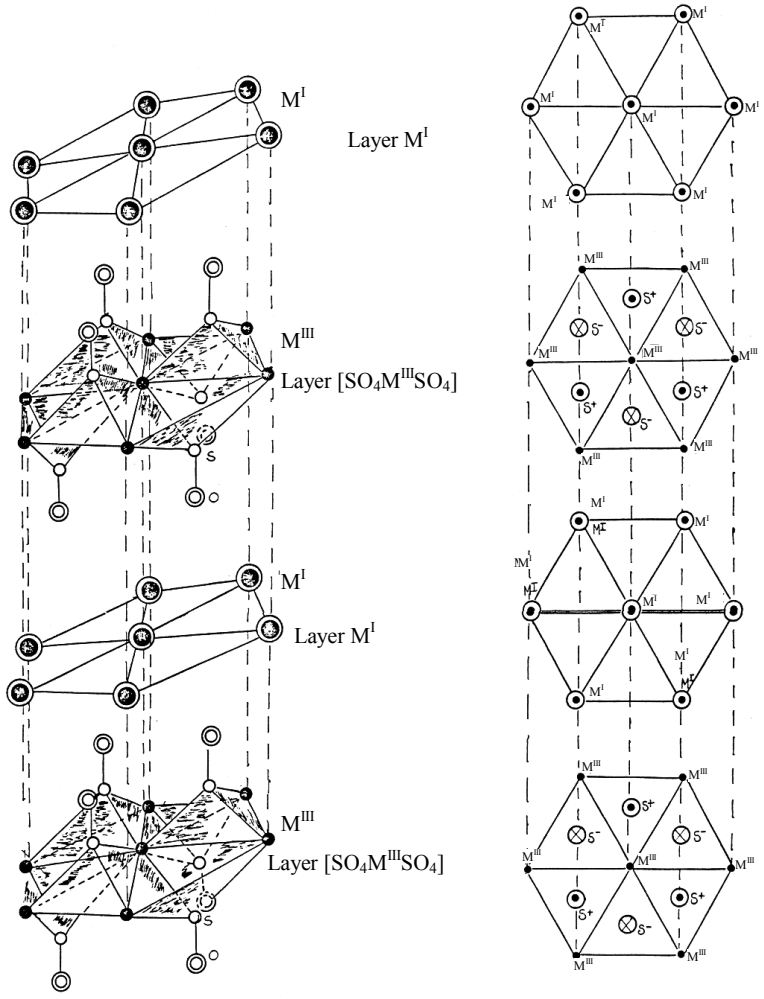


⊙ $S^+$ Sulfur above the plane of $M^{III}$ ions

⊗ $S^-$ Sulfur below the plane of $M^{III}$ ions

**Figure 3.** (b) Hexagonal cells of $M^IM^{III}(SO_4)_2$ stacked along the a and c axes.

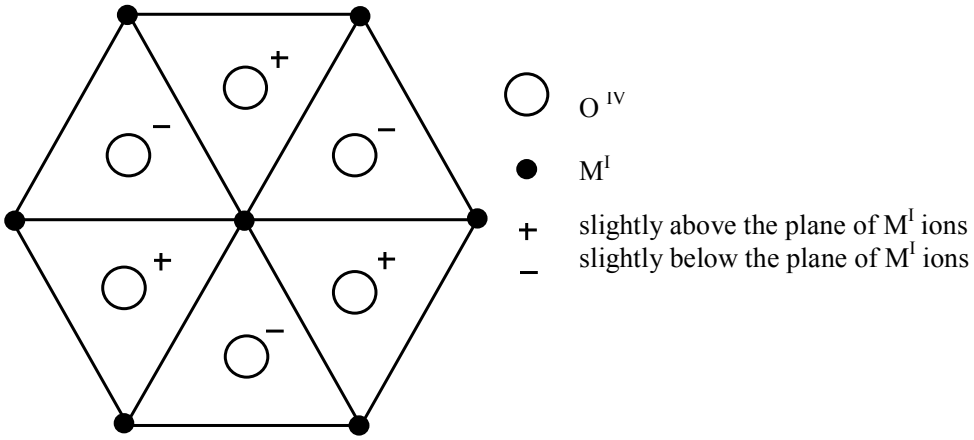


(c)

**Figure 3.** (c) Environment of the $M^I$ ion. The view is parallel to the *c* axis.

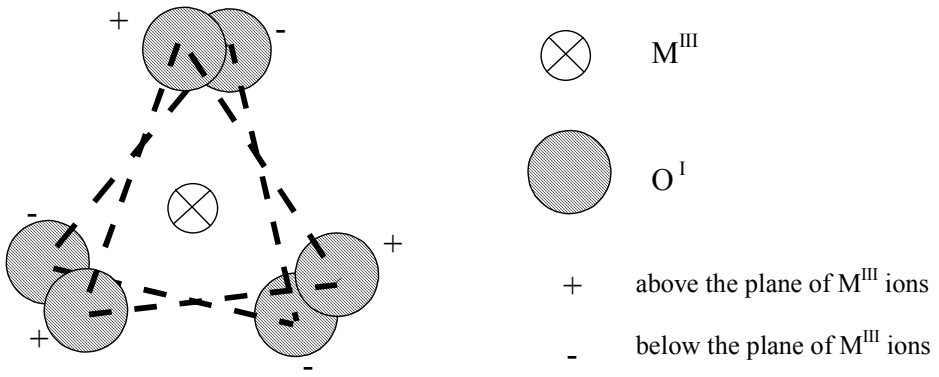


(d)

**Figure 3.** (d) Environment of the $M^{III}$ ions. The view is parallel to the *c* axis.

**Table 1.** Unit-Cell Parameters for $M^IM^{III}(SO_4)_2$

| $M^IM^{III}(SO_4)_2$ | $^a$ (Å) | $^c$ (Å) | Diameter (2*r*) $M^I$ (Å) | $2\Delta r$ $M^I$ (Å) | $\Delta c$ (Å) |
|---|---|---|---|---|---|
| $KAl(SO_4)_2$ | 4.709 | 7.984 | 2.76 | 0.22 | 0.336 |
| $RbAl(SO_4)_2$ | 4.738 | 8.320 | 2.98 | 0.42 | 0.487 |
| $CsAl(SO_4)_2$ | 4.757 | 8.817 | 3.40 | | |
| $KCr(SO_4)_2$ | 4.743 | 8.058 | 2.76 | 0.22 | 0.301 |
| $RbCr(SO_4)_2$ | 4.773 | 8.359 | 2.98 | 0.42 | 0.501 |
| $CsCr(SO_4)_2$ | 4.815 | 8.860 | 3.40 | | |
| $RbFe(SO_4)_2$ | 4.862 | 8.349 | 2.98 | 0.42 | 0.456 |
| $CsFe(SO_4)_2$ | 4.896 | 8.805 | 3.40 | | |

**Table 2.** Reduced Coordinates of $K^+$, $Al^{3+}$, S, $O^I$, and $O^{IV}$ in $KAl(SO_4)_2$ [7]

| Number of position | Wickoff notation of sites | Point symmetry | Atoms | $\frac{x}{a}$ | $\frac{x}{b}$ | $\frac{x}{c}$ |
|---|---|---|---|---|---|---|
| 1 | b | 32 | $Al^{3+}$ | 0.000 | 0.000 | 0.500 |
| 1 | a | 32 | $K^+$ | 0.000 | 0.000 | 0.000 |
| 2 | d | 3 | S | 0.333 | 0.666 | 0.222 |
| 2 | d | 3 | $O^{IV}$ | 0.333 | 0.666 | 0.016 |
| 6 | g | 1 | $O^I$ | 0.016 | 0.672 | 0.317 |

**Infrared Spectroscopy.** The $KAl(SO_4)_2$, $CsAl(SO_4)_2$, $CsCr(SO_4)_2$, and $CsFe(SO_4)_2$. IR bands are summarized in Table 3 [13]. In an isotropic medium, the four internal vibrational bands of the tetrahedral sulfate ion are $\nu_1(A_1)$: 981 $cm^{-1}$, $\nu_2(E)$: 451 $cm^{-1}$, $\nu_3(T_2)$: 613 $cm^{-1}$ and $\nu_4(T_2)$: 1104 $cm^{-1}$ (Only $\nu_3$ and $\nu_4$ are infrared active). The symmetry of the tetrahedral $SO_4^{2-}$ ion is lowered in $M^IM^{III}(SO_4)_2$ because it is on a site with $C_3$ symmetry. Due to a partial reduction of degeneracy, all bands become active in both Raman and I.R. spectroscopy. (See correlation Table 4).

We obtain six IR absorption bands: $\nu_1$, $\nu_2$, $\nu_3$ (1), $\nu_3$ (2), $\nu_4$ (1) and $\nu_4$ (2). (Tables 3 and 4). The frequencies of these bands shift very little versus the specific monovalent ion (comparing $KAl(SO_4)_2$ and $CsAl(SO_4)_2$); however, they strongly depend on the specific identity of $M^{III}$ [viz: $CsAl(SO_4)_2$, $CsCr(SO_4)_2$, and $CsFe(SO_4)_2$]. So, interactions of oxygen atoms in the $SO_4^{2-}$ ions with $M^{III}$ prove to be more significant than with $M^I$. $M^I$–$O^{IV}$ and $M^{III}$–$O^I$ interactions give rise to seven absorption bands. Theses bands are denoted $\nu_5$ to $\nu_{11}$(Table 3). The five band frequencies, $\nu_5$ to $\nu_9$, don't depend on the nature of $M^I$ [viz: $KAl(SO_4)_2$ and $CsAl(SO_4)_2$], but do depend on $M^{III}$ [viz: $CsAl(SO_4)_2$, $CsCr(SO_4)_2$, and $CsFe(SO_4)_2$]. Indeed, these five bands are due to the $M^{III}$–$O^I$ bonds and are observed at relatively high frequencies (500 to 150 $cm^{-1}$).

**Table 3.** Infrared Band Frequencies in $cm^{-1}$ of $M^{I}M^{III}(SO_4)_2$

| | | | | | | | | $\nu_2(E)$ $\delta(OSO)$ 451 | $\nu_4(F_2)$ $\delta(OSO)$ 613 | | $\nu_1(A_1)$ $\nu(SO)$ 981 | $\nu_3(F_2)$ $\nu(SO)$ 1104 | |
|---|---|---|---|---|---|---|---|---|---|---|---|---|---|
| $KAl(SO_4)_2$ | 107 vs | 127 vs | 182 s | 212 w | 280 vs | 387 vs | 500 sh | 473 s | 608 s | 692 s | 1076 w | 1130 vs | 1265 s |
| $CsAl(SO_4)_2$ | 75 vs | 90 vs | 189 s | 214 m | 267 vs | 383 vs | 500 sh | 467 s | 605 s | 686 s | 1073w | 1125 vs | 1250 s |
| $CsCr(SO_4)_2$ | 90 vs | 87 s | 160 vs | - | 243 s | 330 vs | 440 sh | 463 s | 585 s | 668 s | 1050 w | 1067 vs | 1230 s |
| $CsFe(SO_4)_2$ | 70 vs | 85 s | 153 s | 184 sh | 207 s | 260 vs | 380 m | 444 s | 586 s | 655 s | 1030 w | 1060 vs | 1230 s |
| Vibrations | $\nu_{11}$ | $\nu_{10}$ | $\nu_9$ | $\nu_8$ | $\nu_7$ | $\nu_6$ | $\nu_5$ | $\nu_2$ | $\nu_4(1)$ | $\nu_4(2)$ | $\nu_1$ | $\nu_3(1)$ | $\nu_3(2)$ |
| | external vibrations | | | | | | | internal vibrations of $SO_4^{2-}$ ion | | | | | |

vs: very strong; s: strong; m: medium; w: weak; vw: very weak; sh: shoulder

**Table 4.** Correlation Table between $T_d$ and $C_3$ symmetry groups of the $SO_4^{2-}$ ion

| $T_d$ | | $C_3$ |
|---|---|---|
| $\nu_1(A_1)$ | → | A[$\nu_1$] |
| $\nu_2(E)$ | → | E[$\nu_2$] |
| $\nu_3(T_2)$ | → | A + E [$\nu_3(1)$, $\nu_3(2)$] |
| $\nu_4(T_2)$ | → | A + E [$\nu_4(1)$, $\nu_4(2)$] |
| | Activity | |
| $A_1(R)$ | | A(R, I) |
| E(R) | | E(R, I) |
| $T_2(R, I)$ | | |
| | R: Raman active | |
| | I: I.R. active | |

On the other hand, the $\nu_{10}$ and $\nu_{11}$ frequencies depend primarily on the nature of $M^{I}$ [viz: $KAl(SO_4)_2$ and $CsAl(SO_4)_2$] and are not much affected by the nature of $M^{III}$ [viz: $CsAl(SO_4)_2$, $CsCr(SO_4)_2$, and $CsFe(SO_4)_2$]. So, these bands can be assigned to the $M^{I}$–$O^{IV}$ interactions with certainty. The frequencies of these two bands are much lower (130 and 70 $cm^{-1}$) than the $\nu_5$ through $\nu_9$ frequencies (500 $cm^{-1}$ to 150 $cm^{-1}$). Students can conclude that the $M^{I}$–$O^{IV}$ bonds are much weaker than the $M^{III}$–$O^{I}$ bonds, because $M^{III}$–$O^{I}$ interactions are more covalent and $M^{I}$–$O^{IV}$ interactions are mostly electrostatic.

The formal charge on each oxygen ($O^{I}$ and $O^{IV}$) in $SO_4^{2-}$ is equal to –0.5 and that of $M^{I}$ is +1. The positions of the $O^{IV}$ and $M^{I}$ ions, one with respect to the other, near the $M^{I}$ layer (Figure 3c) are such that the formal charge of the ensemble is zero, so that there could be a respective minimization of the electrostatic repulsions and maximization of the electrostatic attractions. These observations confirm the electrovalent character of the $M^{I}$–$O^{IV}$ bonds in these inorganic compounds.

## Conclusion

These X-ray crystallography and infrared spectroscopy studies of $M^{I}M^{III}(SO_4)_2$ lead students to think about: the existence of the $[SO_4–M^{III}–SO_4]^{-}$ layers in the crystallized products; the covalent character of $M^{III}$–O bonds, which assure the cohesion of theses layers; the existence of $M^{I}$ layers between $[SO_4–M^{III}–SO_4]^{-}$ layers, and the electrovalent character of the $M^{I}$–O bond.

This study has been facilitated by the fact that the bonds $M^{I}$–O and $M^{III}$–O are well individualized in the structure of the crystalline compounds $M^{I}M^{III}$ $(SO_4)_2$.

## References and Notes


1. Shoeb Z. E.; Hammad S. M.; Yousef A. A. *Grasas Aceites* **1999,** *50,* 426–434.
2. Redhammer, G. J.; Beran A.; Schneider J.; Amthauer G.; Lottermoser W. *Am. Minéral*. **2000,** *85,* 449–465.
3. Ben Abdelkader S.; Ben Cherifa A.; Kattech I.; Jemal M. *Thermochim. Acta* **1999,** *334,* 123–129.
4. Byeon S. O. *Bull. Koreau Chem. Soc*. **1995,** *16,* 1084–1088.
5. Bukhaloua, G. A.; Mardirosova, I. V.; Ali, M. M. *Zh. Neorg. Khim*. **1998,** *33,* 2511–2514.
6. Eremenko, I. L.; Skripin, Y. V.; Pasynskii, A. A.; Kalinnikov, V. T.; Struchkov, Y.; Aleksandrov, G. G. *J. Organomet. Chem*. **1981,** *220,* 159–164.
7. Vegard, L.; Maurstad, A. *Zeit. Kristall*. **1920,** *69,* 519–532.
8. Franke, W.; Henning, G. *Acta Crystallogr*. **1965,** *19,* 870–871.
9. Bernard, J.; Couchot, P. C. R. *Acad. Sc. C* **1965,** *262,* 209–212.
10. Manoli, J. M.; Kerpin, P.; Pannetier, G. *Bull. Soc. Chim. France* **1970,** *1,* 98–101.
11. Shannon, R. D.; Prewitt, C. T. *Acta Crystallogr,* Sect. B **1969,** *25,* 925–946.
12. Shannon, R. D.; Prewitt, C. T.; *Acta Crystallogr.,* Sect. B **1970,** *26,* 1046–1048.
13. Couchot, P.; Mercier, R.; Perret R.; Bernard J. *Rev. Chim. Min*. **1978,** *15,* 373–396.